Departement für Kleintiere, Klinik für Kleintierchirurgie

der Vetsuisse-Fakultät, Universität Zürich

Direktor: Prof. Dr. Pierre Montavon

Arbeit unter Leitung von Prof. Dr. Keita Ito und Dr. Andrea Tami

A murine delayed-union fracture healing model

Inaugural-Dissertation

zur Erlangung der Doktorwürde der

Vetsuisse-Fakultät Universität Zürich

vorgelegt von

Sandra Wissing

Tierärztin

aus Hagen, Deutschland

genehmigt auf Auftrag von

Prof. Dr. Pierre Montavon, Referent

Prof. Dr. Keita Ito, Koreferent

Zürich 2008

AO Foundation
Research

Department für Kleintiere
Klinik für Kleintierchirurgie
Direktor: Prof. Dr. P. Montavon

AO Forschungsinstitut
Gruppe: Mechano-Biology
Gruppenleiter: Prof. Dr. Keita Ito

A MURINE DELAYED-UNION FRACTURE HEALING MODEL

vorgelegt von

Sandra Wissing

TABLE OF CONTENTS

Summary 4

Introduction 5

Material and Methods 8

Mouse Model 8

Osteotomy and periosteal injury 9

Mechanical Testing 10

Micro-CT 12

Regions of interest (ROI) 13

Radiographic score 15

Histology 16

Statistics 17

Results 18

Mechanical Testing 18

Micro-CT 19

Radiographic score 25

Histology 26

Discussion 35

References 39

Acknowledgments 43

SUMMARY

As the murine genome has been mapped, a murine delayed union model of fracture healing would be appealing to understand the molecular mechanisms and treatments for this still persistent complication. Due to the important role played by the periosteum in perfusion of bone during fracture healing and as source of progenitor cells, we investigated the effect of a standardized periosteal injury on healing of a gap osteotomy in this study to determine if it would eventually lead to a delayed union. Results from the micro-CT and immuno-histological evaluation showed that periosteal injury suppressed callus growth significantly and induced a delay in woven bone formation and its subsequent remodeling into lamellar bone. Radiographical grading indicated a temporal shift in healing of up to 2 weeks. Stiffness of the healing bones was also significantly lower for the periosteal injured group. However, despite delay, bone healing did continue albeit slower than in the control. In conclusion, this mouse model based on periosteal injury can be used in the future to evaluate basic research question regarding delayed unions such as involvement of certain pathways or genes. Moreover, it can enable the development of further diagnostic tools and treatment options.

INTRODUCTION

Fracture healing is a process of bone regeneration which recapitulates fetal osteogenesis processes of endochondral and intramembranous ossification [1,2,3]. It is a complex procedure including differentiation, proliferation, migration and apoptosis of several mesenchymal cell types [4]. These and other cells communicate via growth factors and cytokines [5] synthesizing matrix proteins as well as matrix remodeling enzymes [6] and angiogenic stimulators. This biological cascade is coordinated to restore mechanical stability and thus functionality of the fractured bone. Depending on the method of fixation, primary or secondary healing will occur. Less-stabilized fractures pass through endochondral and intramembranous ossification, whereas more rigidly stabilized fractures heal by osteonal remodeling and sometimes intramembranous ossification [7].

One of the complications which can appear during fracture healing is the development of a delayed union which occurs with an incidence of 5 to 10% [8,9]. A delayed union is described as a fracture which has not undergone union in the expected physiological time [10] and therefore healing time is prolonged. Usually, treatment includes a secondary operative intervention which is often associated with significant economic impact and patient morbidity [11]. Delayed unions play an important role in the pathophysiology of fracture healing because the reasons for their appearance are not completely clarified yet [12].

Interfragmentary instability represents one of the most important factors for the development of delayed unions [10,13,14]. Nevertheless, adequate load is necessary for angiogenesis and osteogenesis [15]. Furthermore, inadequate blood supply during fracture healing is also a major reason for the appearance of delayed unions

[10,14,16,17]. A fracture disconnects the vascular channels followed by acute necrosis and hypoxia of the adjacent bone and marrow [14]. Usually, the medullary and the metaphyseal vessels are disturbed by a fracture and their function is carried over by periosteal and extraosseous arteries via increase of blood flow and by changing their blood flow patterns until normal blood supply is restored [10,18]. The loss of periosteal soft- tissue attachments lead to absence of blood supply in bone and to a failure of bone healing [19]. Consequently, the recruitment of additional periosteal and extraosseous arteries is very important in the initial phase of fracture healing [20] to achieve bone union.

In an attempt to identify potential targets for biochemical diagnosis and intervention of delayed unions, it would be very helpful to first elucidate the physiological and pathophysiological mechanisms. However, for this purpose and due to the biological complexity of fracture healing, well-standardized animal models of delayed fracture healing are required. In the literature, not many animal models can be found, but murine models are already established in research for studying bone biology and skeletal repair because the mouse genome is entirely known [14]. This fact involves the possibility to develop knockout mice for molecular biology based investigations [21]. Furthermore, murine models are cheap and easy to handle [22]. El-Zawawy et al. already created a delay in fracture healing in a smoking mouse model [23]. Holstein et al. investigated the effect of rapamycin treatment on fracture healing in a mouse model and achieved an initial delayed union. Other recent studies dealt with specific deficiencies in mice, like osteopontin- or interleukin-6- deficiency [24,25], which also created a delay in bone healing. However, all these murine models led to a special pathophysiology and therefore cannot correspond to the appearance of

delayed unions in general because these particular models are not able to identify general targets. Therefore a general mouse model of delayed union is lacking.

In a previous study [26] a murine model of delayed union based on interfragmentary instability was investigated. Using a flexible internal fixator, secondary healing was induced similar to that seen in human diaphyseal fracture healing. However, the results of that project showed that interfragmentary instability in combination with a moderate gap was not sufficient to obtain a significant delay in bone healing. Therefore, in the current study we hypothesized that an additional intervention in the form of a periosteal injury could lead to a more substantial delay in the healing cascade. For this purpose the periosteum was cauterized in close proximity to the osteotomy gap and bone fragments were internally fixed in a flexible arrangement with a rigid plate and partially locked screws [27,28]. The successful development of this murine model will enable further studies to elucidate the mechanisms involved with delayed fracture healing.

This project was divided into two parts: The surgery and the micro-CT scanning were carried out by Dr. Ina Dorothee Groengroeft and my part was the micro-CT data evaluation and the histological work.

MATERIAL AND METHODS

Mouse model

For this project 120 C57BL/6 mice at the age of at least 20 weeks (RCC Ltd, Füllinsdorf, Switzerland) were used and kept in group cages under day and night light regime (12 hours light and 12 hours dark). These accommodations were enriched with objects, e.g. a Mouse House™ (Tecniplast Deutschland GmbH, Hohenpeißenberg, Germany). Permanent access to water and diet (Provimi, Provimi Kliba AG, Kaiseraugst, Switzerland) were guaranteed. The Animal Experimentation Commission of the Veterinary Office of the Canton of Grison, Switzerland permitted all methods and treatments which were applied in this project. Furthermore, the routines of this study were accomplished according to the guidelines of the Swiss Federal Veterinary Office for the use and care of laboratory animals. On all mice a mid-diaphyseal osteotomy of the left femur was performed and they were divided randomly into two groups (with or without periosteal injury). This injury was inflicted by cauterization of the periosteum. Animals were sacrificed either at 1, 7, 14, 21, 28 or 42 days post surgery by CO_2 inhalation (n = 10 mice / treatment group / time-point). Post-mortem lateral view radiographs were taken. The femora were explanted and freed from soft tissue. Immediately after their explantation non-destructive mechanical tests were performed. Subsequently, samples were scanned with a micro-computed tomography (micro-CT) system. Finally, qualitative histological analysis was carried out.

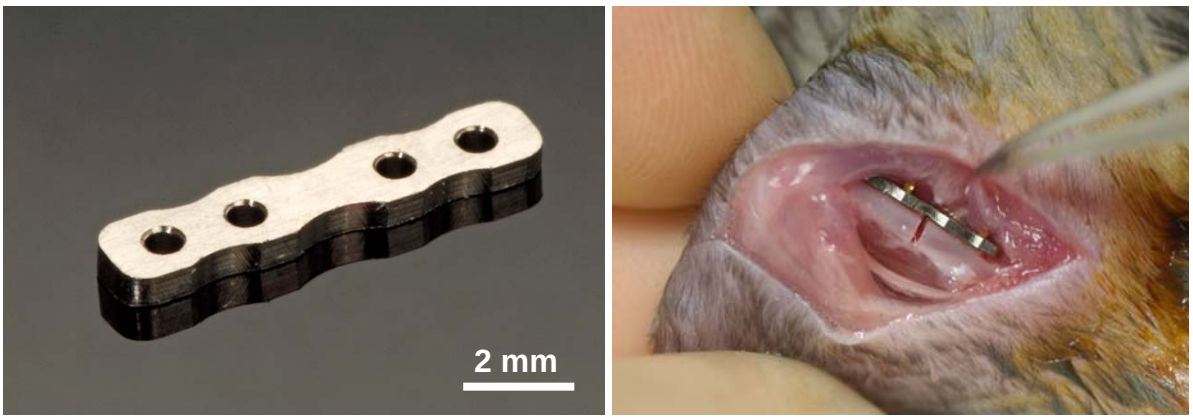

Figure 1: Rigid MouseFix™ plate (LEFT). Plate in situ after implantation (RIGHT).

Osteotomy and periosteal injury

The anesthesia was initiated in an induction chamber with 5% Isofluran and 100 ml/min O_2. During surgery, the mice were kept constantly under general anesthesia with 2% isofluran (Isofluran Baxter ad us. vet.®, Baxter AG, Volketswil, Switzerland) at 200 ml/min O_2 via mask. Animals were kept in a prone position and the surgical approach was performed on the lateral side of the femur between Musculus vastus lateralis and Musculus biceps femoris by longitudinal incision. Femur was prepared at the transition from the mid third to the proximal third. In the group with periosteal injury a cautery foil (0.8 mm thick) was pulled tightly around the bone. An electrotome was slided over both ends of the foil and the periosteum was cauterized for 0.5 sec. A standardized 1 mm wide thermal periosteal injury was created. Constant intensity and burning depth were used for all bones so that the whole periosteum in that defined region was destroyed. The cautery foil was then removed and a rigid MouseFix™ plate was fixed onto the femur with two screws in each bone fragment. Subsequently, a 0.45 mm gap osteotomy was accomplished at the mid-diaphysis in using a gigly saw under continuous irrigation. Accordingly, the periosteal injury

included approximately a width of 0.275mm proximal and distal adjacent to the fracture gap. Thereafter, screws were loosened for ½ turn to reduce fixation stability and induce secondary healing. The wound was closed in three layers (Vicryl® & Ethicon®, Johnson & Johnson Intl, St-Stevens-Woluwe, Belgium) and covered with skin staples to avoid wound biting. Lateral view radiographs were taken. As analgesia mice received 0.1 mg/kg buprenorphine subcutaneous every 10-14 hour (Temgesic®, Essex Chemie AG, Lucerne, Switzerland) for 2 days. Afterwards, paracetamol was administered per os for 5 days (Dafalgan Sirup für Kinder®, 7 ml in 103 ml cold water as drinking water; UPSAMEDICA GmbH, Baar, Switzerland). Immediately after recovering from surgery mice were allowed to freely move and fully load the operated leg.

Figure 2: Mouse bone before (LEFT) and after (RIGHT) periosteal injury caused by cauterization.

Mechanical Testing

Femora of both treatment groups at time-point 21, 28 and 42 days were tested mechanically to measure bending stiffness using a BOSE testing device (EL 3220,

Bose Corporation- Electro Force Systems Group, Eden Prairie, Minnesota, USA). Bones from earlier time- points (i.e. 1, 7, 14 days) were not tested due to insufficient healing. Under continuous hydration with Ringer's lactate samples were tested in non-destructive 4pt-bending. The same procedure was also done with the intact femora of the contra-lateral side of these mice. Samples underwent 3 loading sequences, each consisting of 2 loading cycles, one for preconditioning and one for stiffness measurement. After each loading sequence, bones were first removed from the 4pt-bending holder and then repositioned. Femora were load under displacement control at a cross head rate of 0.1mm/min (deformation rate of 2.1deg/min). The compression side corresponded to the former plate position. Maximal applied force was -3.5N. Bending stiffness was calculated using the linear portion of the curve between -2.5 and -3.5N. The mean bending stiffness of each osteotomized femur obtained from the 3 loading sequences was normalized to the contra-lateral intact femur.

Figure 3: 4-point-bending jigs to accurately test the femur with the loading device.

Micro-CT

All explanted femora, some after mechanical testing, were first fixed for one day in 4% buffered formalin, washed in water and stored in 40% ethanol before being measured using a micro-CT scanner (µCT40®, SCANCO Medical, Brüttisellen, Switzerland). The X-ray tube was operated at 70 kVp and 114 µA with an integration time of 200 ms and the long axis of the femur was aligned orthogonally to the axis of the X-ray beam. This position was maintained in a custom-made holder by two pins which were implanted in the most proximal and distal screw holes of the bone. The volume between the two pins was scanned with 400 2-dimensional transverse cross-section images and reconstructed in 1024 x 1024 pixel matrices from 400 projections at a nominal spatial resolution of 12 μm. For monitoring the fracture healing process and accurately differentiating the effect of periosteal injury several regions of interest (ROI) were defined within the two outermost plate screws on each side of the osteotomy gap (cp. next paragraph). A 3D Gaussian filter with a sigma of 0.8 and a support of one voxel was used to partly suppress the noise. The ROIs were processed with a threshold procedure [29] that allowed the segmentation of woven bone (less mineralized) and mature, lamellar bone (more mineralized), and the calculation of the corresponding sub-volumes. Threshold values were set to 14.5% for woven, less mature bone (low attenuation) and 36.0% for lamellar, more mature bone (high attenuation, in percent of maximal image grey value) based on previous comparison with histological sections.

Regions of interest (ROI)

For precise quantitative analysis different ROIs were defined and manually contoured (Figure 4). The first ROI, i.e. the total region of interest (TOT) was the largest one and included the entire scanned volume between the two outermost plate screws on each side of the osteotomy gap. Instead, the periosteal region (PER) comprised any new bone tissue starting at the outer cortical boundary of the femora and extending radially outward, while the endosteal region (END) contained all newly formed bone within the medullary cavity, i.e. within the inner cortical boundary of both fragments. The most important ROI in this study was the actual fracture gap (GAP) which was defined as the space between both fragments and its extension in radial direction (Figure 4, BOTTOM). The gap zone had to include only newly formed tissue. Any bone fragments and original mid-diaphyseal cortex were excluded (Figures with real bone cross-section).

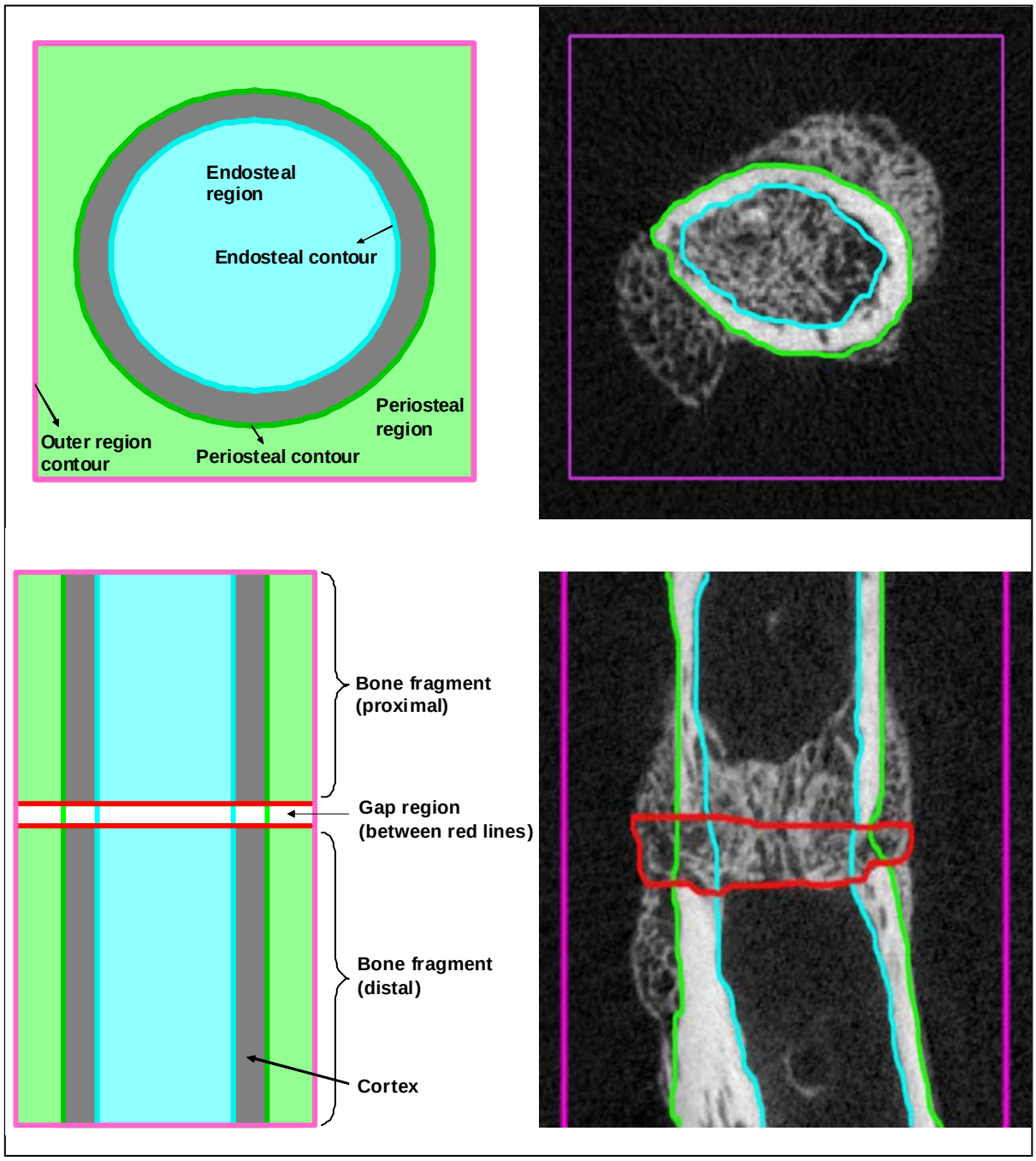

Figure 4: Cross-section (TOP) and longitudinal section (BOTTOM) with the contours drawn for the quantitative evaluation of new bone formation and maturation. (LEFT: schematic illustration; RIGHT: real CT-images).

Radiographic score

Blinded postoperative and post-mortem radiographs as well as cross-sectional CT images were graded based on callus formation and rebridgement of the cortices and remodeling processes using the radiographic scoring scale of Garret et al. [30] (cp. Table). Radiographs provided the overview of fragment alignment and callus formation, while 16

2-dimensional CT-cross-sections equally spaced in the central part of the gap region (2.45 mm length including the osteotomy gap and 1mm of each bone fragment) were assessed blindly by one investigator with medical experience.

0	No bridging, no callus formation
1	No bridging, initiation of a small amount callus
2	No bridging, obvious initial callus formation near fracture
3	No bridging, marked callus formation near and around fracture side
4	Rebridging of at least one of the cortices, marked callus formation near and around fracture side
5	Rebridging of at least one of the cortices, marked and complete callus formation around fracture side
6	Rebridging of both cortices, and/or some resolution of the callus
7	Clear rebridging of both cortices and resolution of the callus

Table 1: Radiographic scoring scale [30].

Histology

For histological qualitative analysis femora of both treatment groups at time-point 14 to 42 days were stored in special cassettes in 40% ethanol. These cassettes contained two nets (one at the top and one at the bottom of the mold) (Figure 5) that allowed precise and stable positioning of the bones during the decalcification and embedding procedure and for the subsequent cutting protocol of mid-sagittal sections. Samples were washed in water and decalcified in 12.5% EDTA (Schweizerhall Chemie AG, Basel, Switzerland) at room temperature for 13 days. After additional washing in water and dehydration in an ascending series of ethanol concentration (2x 50%, 2x 70%, 2x 96% and 2x 100% ethanol), samples were first transferred to xylene and afterwards embedded in paraffin and serially cut in slices with a thickness of 6μm using a microtom (HM 3555 S, Microm International GmbH, Walldorf, Germany). Immunohistochemistry was performed for collagen II (CIICI developed by Holmdahl and Rubin, Developmental Studies Hybridoma Bank, NICHD, University of Iowa, Department of Biological Sciences, Iowa City, IA, USA) and collagen X (polyclonal rabbit antibody, kindly provided by Prof. D. Chang, University of Hong Kong, Dept. of Biochemistry, Hong Kong SAR, China) to compare the time course of chondrocytes maturation and differentiation. Staining for collagen II was accomplished with the Vectastain M.O.M.™-Kit Peroxidase (Vector Laboratories Inc) and the Vectastain Peroxidase Substrate Kit DAB™ (Vector Laboratories Inc, Burlingame, CA, U.S.A.). Instead, staining for collagen X was performed with the Vectastain Elite ABC Kit and with the Vectastain DAB™ Peroxidase Substrate Kit (Vector Laboratories Inc, Burlingame, CA, U.S.A.). Additionally, immunohisto-stainings were counterstained with Haematoxylin and Eosin (Fluka, Buchs, Switzerland) to provide clearer overview images. For better

differentiation between cartilage and fibrous tissue sections were also stained with Toluidine blue (Fluka). Afterwards the sections were evaluated qualitatively with the Axioplan® Imaging 2 microscope and Axiovision software (Carl Zeiss AG, Feldbach, Switzerland) by using transmitted light with 50x and 100x magnification.

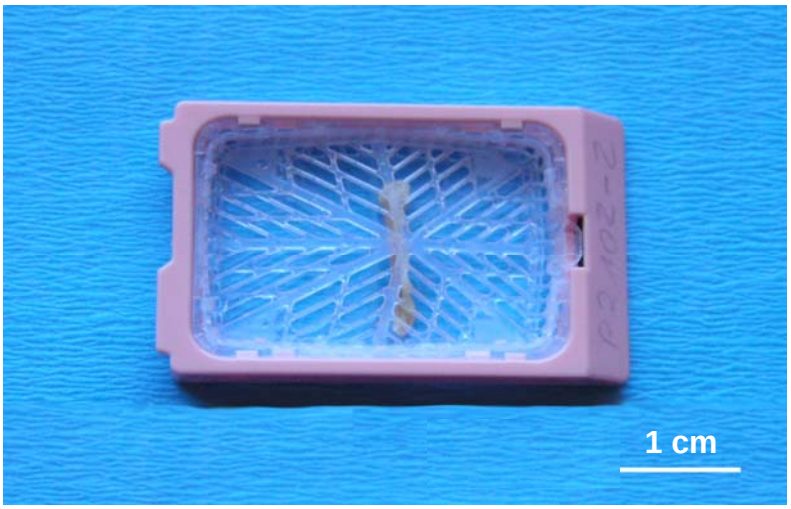

Figure 5: Embedding cassette with mouse bone sample.

Statistics

Analyses of the quantitative micro-CT results were carried out using SPSS software (SPSS Science, 14.0 for Windows Chicago, IL, USA). A p-value of 0.05 was used as a threshold for statistical significance. Normal distribution was determined with Shapiro-Wilk test. An analysis of variance was performed with periosteal injury and healing time as factors in a full factorial general linear model using a Tukey correction for post-hoc testing. In the case of significant interaction between the two factors, a One-Way ANOVA for “time” and an independent T-test for “treatment” were performed separately. For the radiographic scoring differences between groups were analyzed using the nonparametric Kruskal–Wallis test.

RESULTS

Mechanical testing

Stiffness of the healing bones at 21, 28 and 42 days post-surgery was significantly lower for the periosteal injury group compared to the control group at each time point ($p < 0.03$). Furthermore, stiffness increased over time in both groups, whereby at 42 days it was significantly higher than at previous time points ($p=0.001$) (Figure 6).

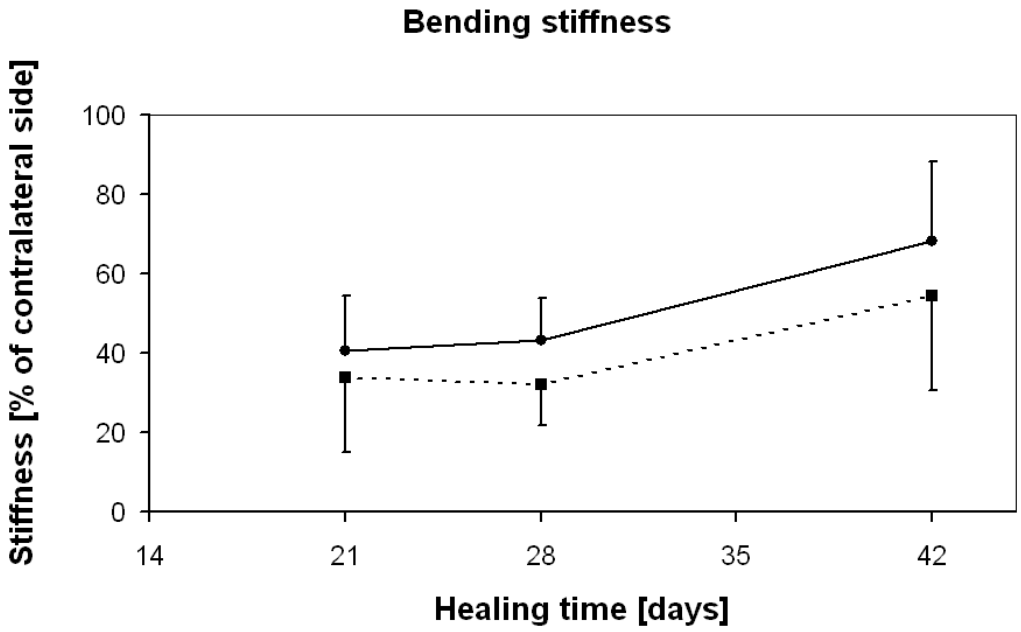

Figure 6: Bending stiffness of all osteotomized femora (mean ± SD) normalized with the contra-lateral intact femora (— = control group, - - - = group with periosteal injury).

Micro-CT

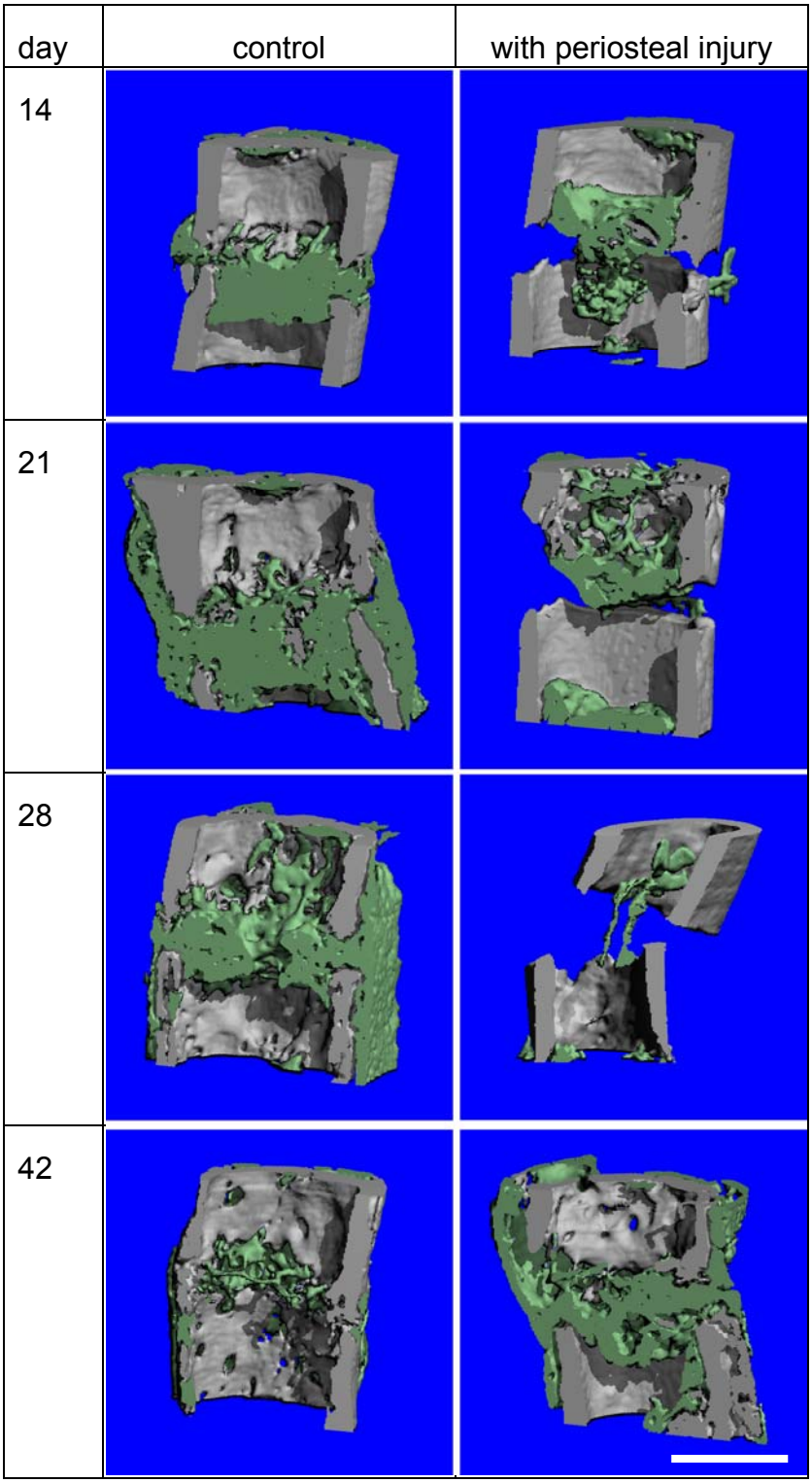

Figure 7: Reconstructed 3-dimensional images. Segmentation of highly mineralized (gray) and lowly mineralized (green) tissue within the scanned volume (scale bar = 1 mm).

TOT

Quantitative micro-CT evaluation of the ROI “TOT” showed that treatment had an influence on the healing response, whereby periosteal injury impaired and reduce the amount of woven bone formed during the healing process (Figure 8). In both groups the amount of woven bone changed significantly over time ($p < 0.001$) and increased from day 7 to day 21. In the group without periosteal injury a substantially steeper rise in woven bone formation was recorded, especially between 14 and 21 days. At time-point 21 days the curve of the control group reached a clear maximum ($p = 0.005$). In contrast, the amount of woven bone in the group with periosteal injury increased at a lesser, steady rate until day 28. At that time-point the curve peaked less obviously and was significantly different compared to day 7 and 14 ($p < 0.025$). Thereafter, the amount of woven bone decreased in both groups until the end of the experimental period. The volume of lamellar bone for TOT, which comprises the lamellar bone from the mid-diaphyseal cortices of the distal and proximal bone fragment, stayed at a rather constant value and did not show any significant changes during the healing period and between both treatment groups.

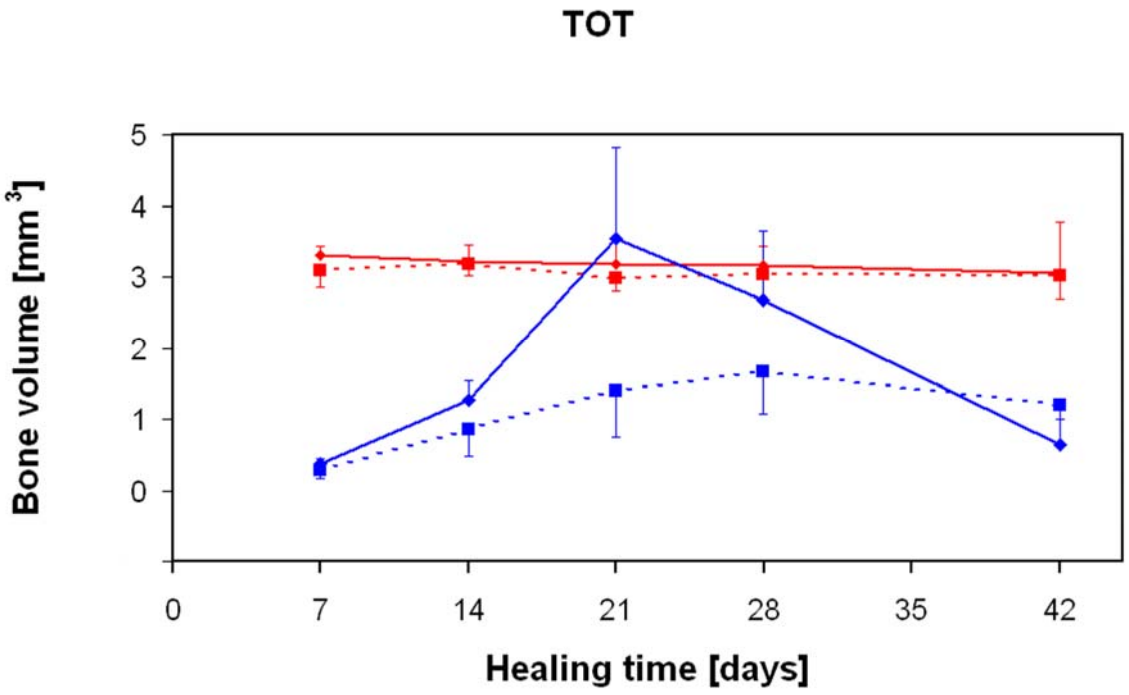

Figure 8: Total amount of lamellar and woven bone during the healing period (mean +/- SD) (red: lamellar bone; blue: woven bone; —: control group; - - -: group with periosteal injury).

PER

Given the fact that during fracture healing of long bone most of the callus material is formed around the original cortical boundary of the fragments, the quantitative micro-CT results for woven bone in the ROI “PER” (Figure 9) largely match the outcome observed for the ROI “TOT”. The amount of woven bone in both groups changed significantly over time ($p < 0.001$). In the group without periosteal injury at day 21 there was again an evident peak in woven bone formation ($p < 0.001$), while in the periosteal injured group at the same time point significant increase ($p < 0.018$) had just started and to a much smaller degree. The amount of lamellar bone began to

slowly increase at day 14 in both groups, but it increased significantly only at day 42 ($p < 0.046$).

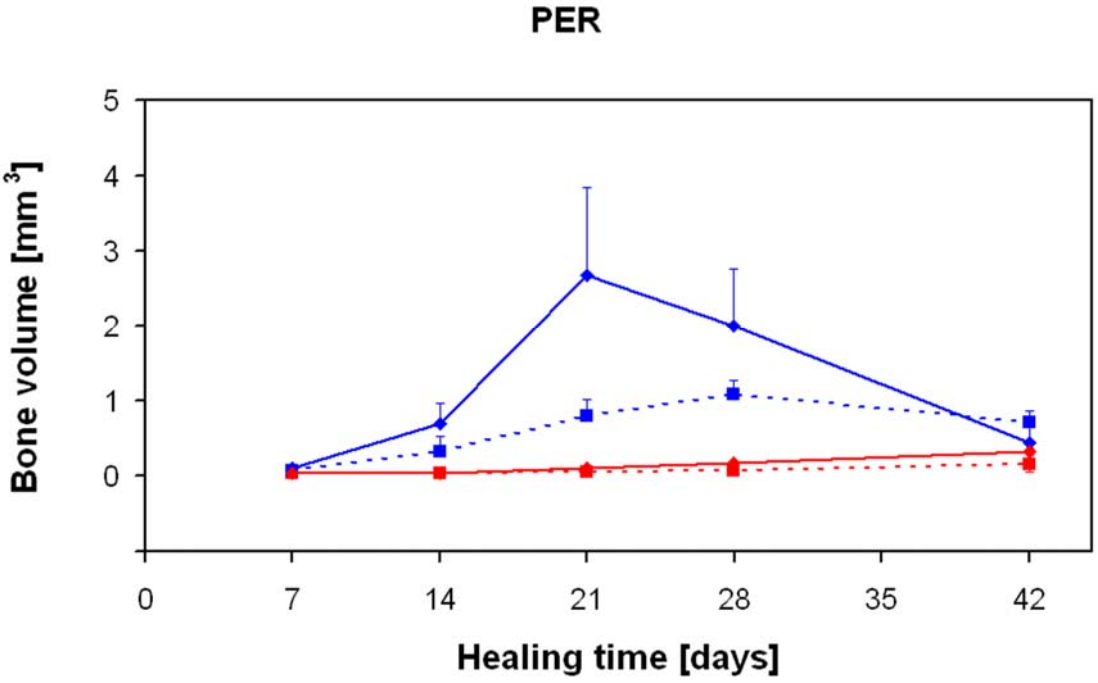

Figure 9: Amount of lamellar and woven bone during the healing period in the periosteal region (mean +/- SD) (red: lamellar bone; blue: woven bone; —: control group; - - -: group with periosteal injury).

END

As expected, for the ROI “END” (Figure 10) the amount of woven bone is clearly less compared to the above analyzed regions of interest “TOT” and “PER”. However, similar patterns of callus formation and remodeling are recognizable. Woven bone volume in the control group changed significantly over time ($p < 0.049$): it first increased, reaching a peak at 21 days and subsequently decreased until the end of the experimental period. In contrast, no peak was recognizable for the periostal

injured group over time, whereby the amount of woven bone increased significantly ($p < 0.010$) from day 7 to a plateau value that stayed constant between day 14 and 28. Finally it decreased slightly towards day 42. The amount of lamellar bone remained more or less constant. In the control group the curve increased a little between 7 and 28 days ($p < 0.002$), then it decreased up to day 42 ($p < 0.045$). In the group with periosteal injury the amount of lamellar bone increased very slightly over the whole experimental time and only at day 42 it was significantly higher ($p < 0.046$).

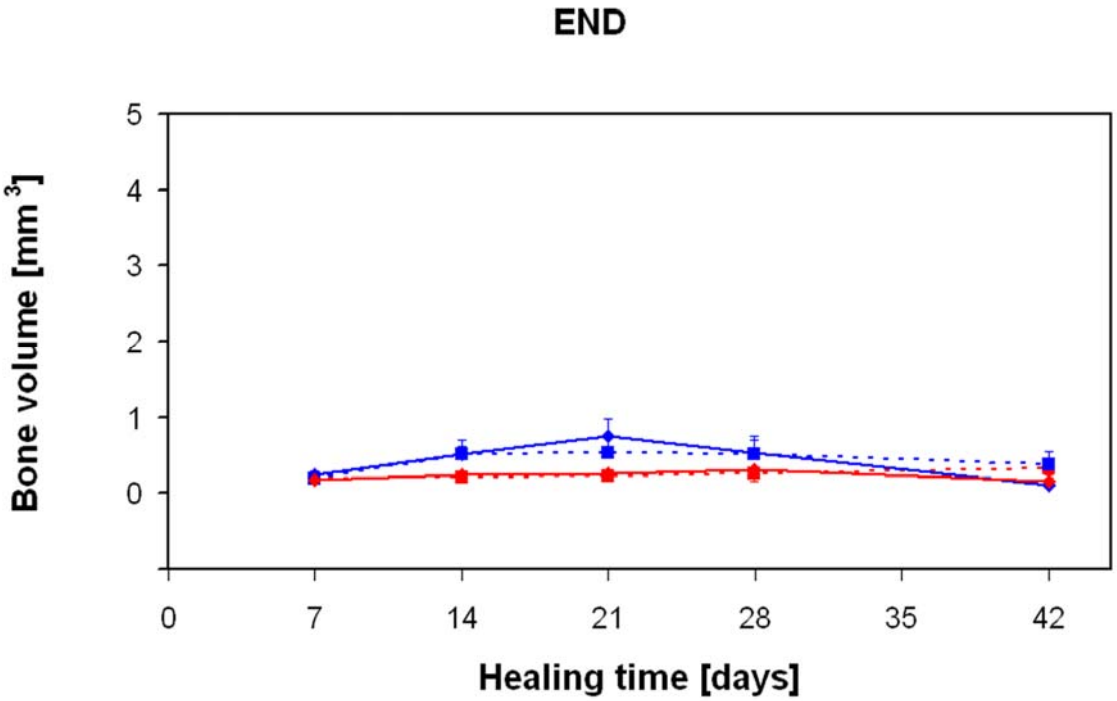

Figure 10: Amount of lamellar and woven bone during the healing period in the endosteal region (mean +/- SD) (red: lamellar bone; blue: woven bone; —: control group; - - -: group with periosteal injury).

GAP

As already noted for the other regions of interest the periosteal injury suppressed callus growth in the ROI “GAP” resulting in significantly less woven bone formation ($p < 0.034$) compared to the control side (Figure 11, note: y-axis is scaled). The amount of woven bone in the group without periosteal injury increased to a peak from 7 to 21-28 days ($p < 0.001$). Thereafter, woven bone volume decreased significantly towards day 42. Instead, in the group with periosteal injury woven bone increased from day 7 to day 21 and 28. However, significant changes resulted only after 42 days ($p < 0.047$). No significant changes were measured between day 21 and 42 ($p > 0.805$): in this time frame an unstable pattern of increase and decrease was evident. Lamellar bone volumes increased significantly on the control side ($p = 0.003$) by the end of the experiment, while no significant changes resulted in the presence of periosteal injury ($p = 0.120$).

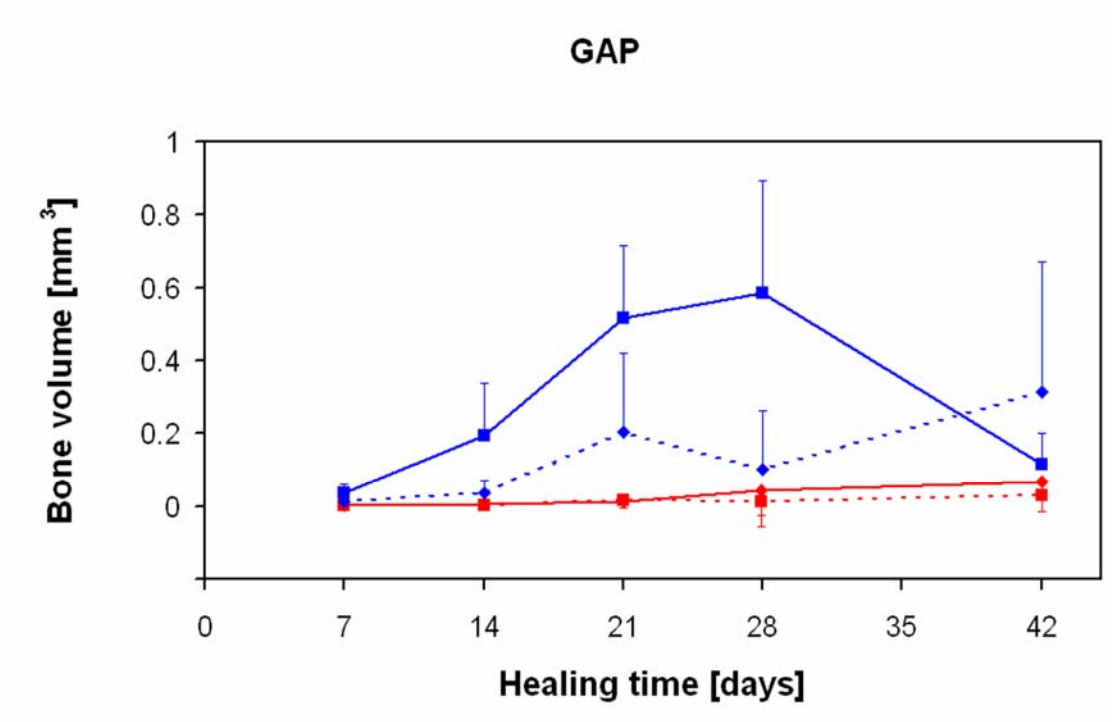

Figure 11: Amount of lamellar and woven bone during the healing period in the gap region (mean +/- SD): (red: lamellar bone; blue: woven bone; —: control group; - - -: group with periosteal injury)

Radiographic score

Radiographical grading for the control side indicated earlier more advanced healing over time compared to the side with periosteal injury. The delay in score magnitude ranged between approximately 1-2 weeks. In both groups a significant increase in scoring resulted from day 7 to 14 ($p < 0.022$) and from day 28 to 42 ($p < 0.024$). However, while in the control group the scoring exhibited a constant increase between day 14 and 28, over the same period a higher variability in healing progress was registered in the group with periosteal injury. Comparing the groups at the same time points, starting at day 14 the scoring in the control group was always

significantly higher than in the injured group ($p < 0.028$), in which rebridgement had not yet been attained after 42 days.

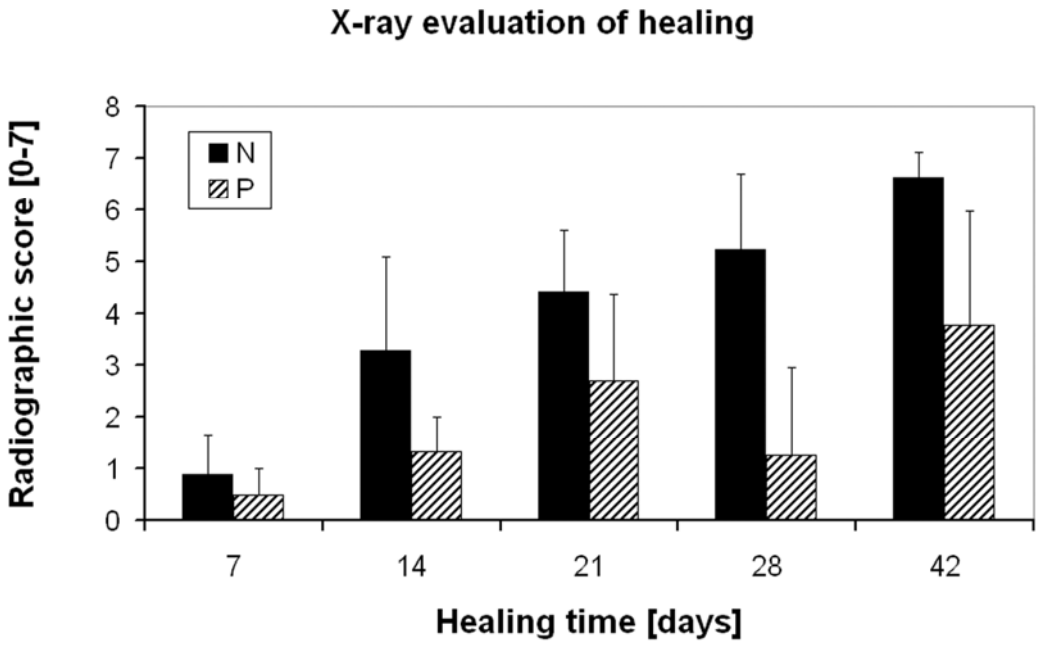

Figure 12: Radiographic score callus formation and cortical bridging assessed blindly by one independent investigator using a scoring scale based on rebridgement of the cortices and acceleration of healing (based on the scale presented in Table 1.

Histology

Histological results corroborated the quantitative outcome from the micro-CT analysis. Based on the expression of collagen II (Col II) and collagen X (Col X), on the formation and resorption of cartilaginous tissue in the gap and on the rebridgement of both fragments, the healing course was clearly prolonged in the group with periosteal injury. In control bones a more robust expression of Col II and Col X was observed between 14 and 28 days. After 14 days the callus in the fracture

gap area consisted of woven bone in combination with cartilage which was mainly located in the centre of the gap region. At day 21 a more massive periosteal reaction was visible, whose cartilaginous portion was increasingly replaced by woven bone as evidenced by the intense Col X signal. In contrast to day 14 cartilage formation was located predominantly at both sides of the fracture gap. First signs of cortical bridging by woven bone were recognizable (Figure 12 to 17). At day 28 both cortices were bridged with woven bone and remodeling had already started, noticeable by the advanced stage of callus resorption around the periosteum and in the endosteal cavity. In the group with periosteal injury, woven bone formation and the amount of cartilage was delayed which was demonstrated by the expression of Col II and Col X. After 14 days just connective tissue and no callus was visible in the fracture gap. At day 21 Col II and Col X were detected representing the amount of cartilage which was present only within the cortical boundaries of the two fragments (i.e. no periosteal reaction). Fibrous tissue was also visible. Woven bone formation, originated from the proximal endosteal cortices, started to fill the gap. Suddenly, after 28 days an extensive cartilaginous callus was built on one side of the fracture which also included a mild amount of woven bone: this may reflect a late reaction to a persistent instability of the fracture fixation and mechanically inadequate reaction with fibrous tissue and cartilage. Due to the massive periosteal reactions the state at this time-point was similar to the situation at day 21 in the control group.

In general, the results from the immunohistochemistry demonstrated that in the control group the normal course of chondrocyte maturation and subsequent hypertrophy characteristic of endochondral ossification took place. Between 2 and 4 weeks after osteotomy the amount of woven bone built in the gap region first increased and then started to resorb gradually. During the same time span the

amount of cartilage steadily decreased. Instead, in the group with periosteal injury, very little reactions were noticeable at the beginning: fibrous connective tissue was present for a longer time in the gap and a cartilaginous stable callus was still missing after 4 weeks, when eventually healing seemed to start its normal course.

day	control group	with periosteal injury
14	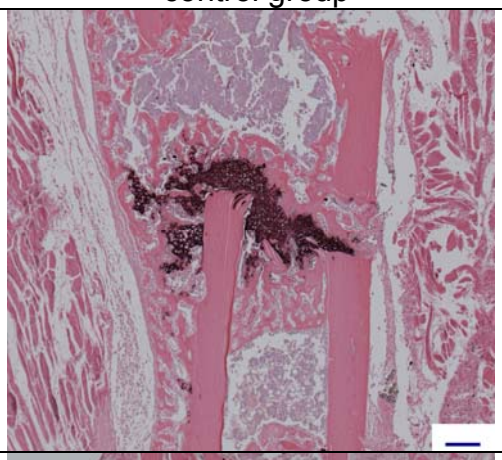	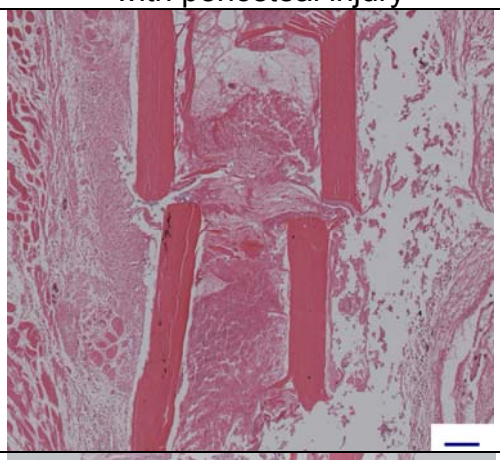
21	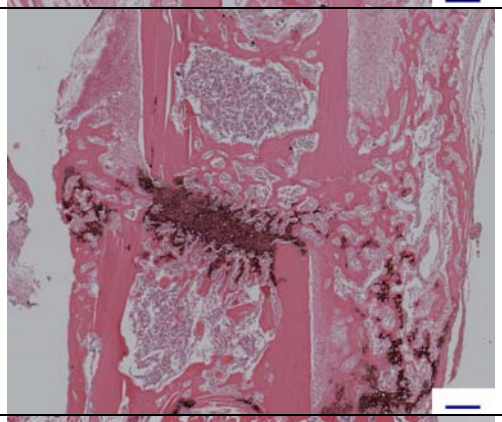	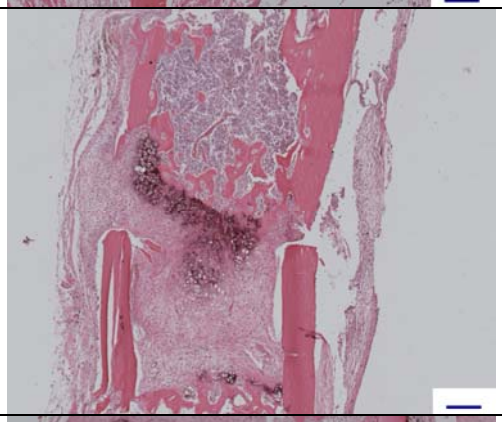
28	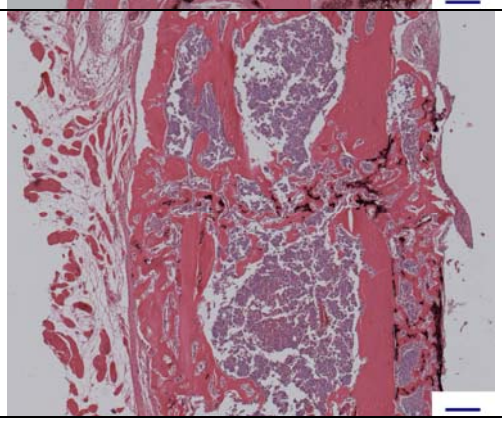	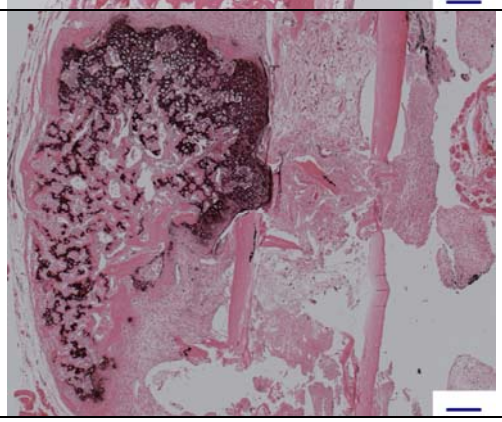

Figure 12: Histology of mid- sagittal section through the osteotomy gap, stained with collagen X + Haematoxylin / Eosin (50x magnification), (blue scale bar: 200 µm).

day	control group	with periosteal injury
14	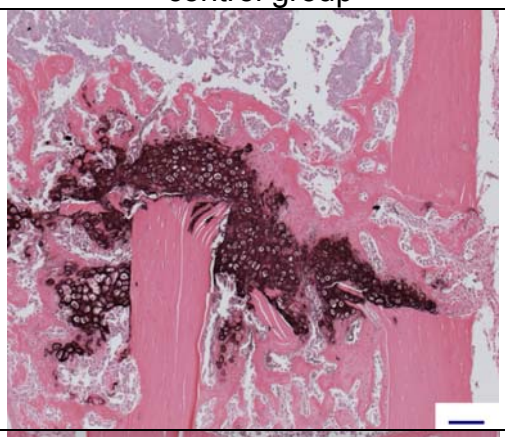	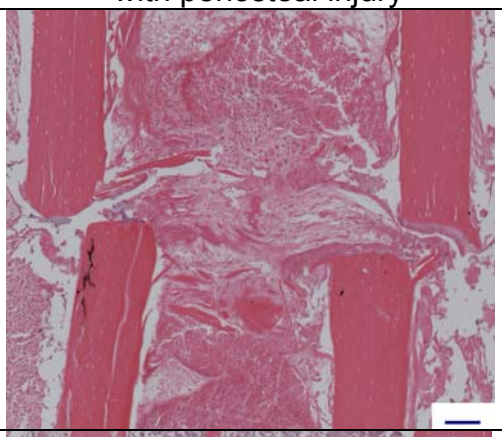
21	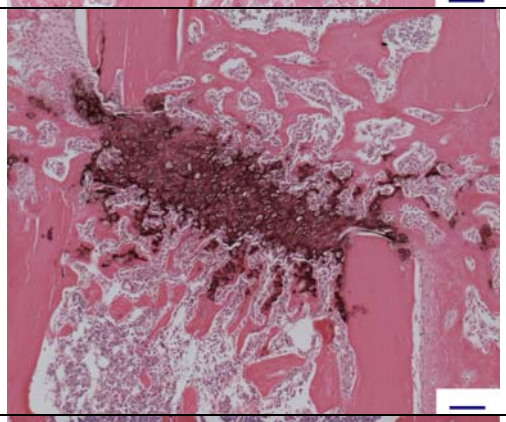	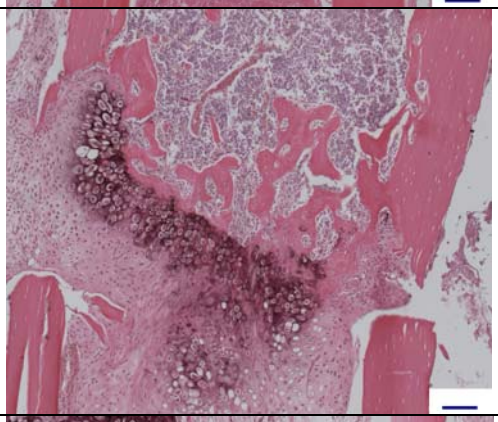
28	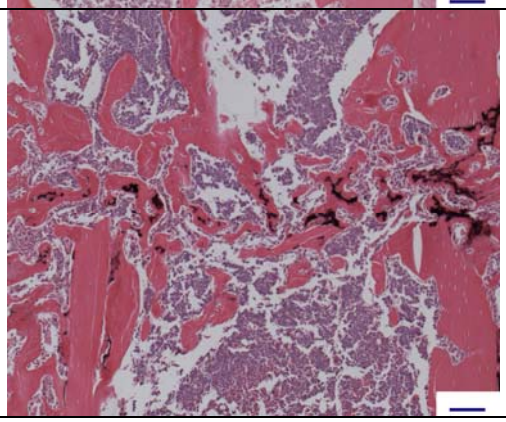	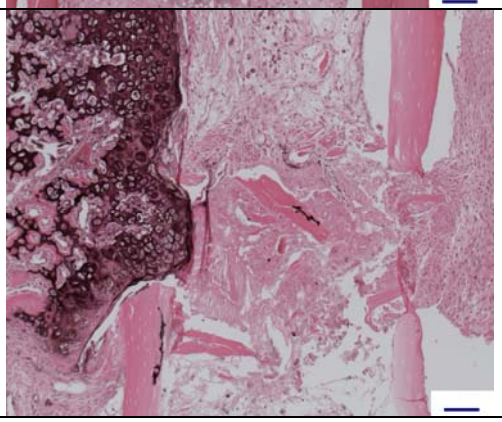

Figure 13: Histology of mid- sagittal section through the osteotomy gap, stained with collagen X + Haematoxylin / Eosin (100x magnification), (blue scale bar: 100 µm).

day	control group	with periosteal injury
14	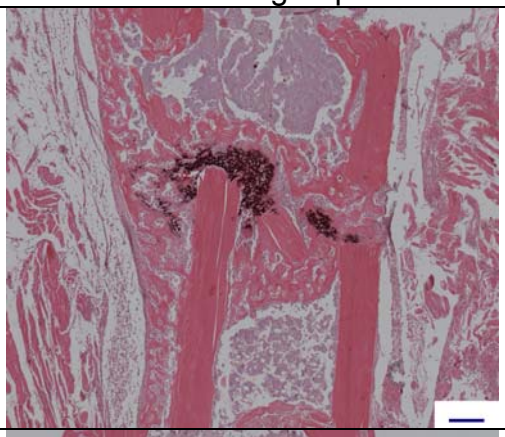	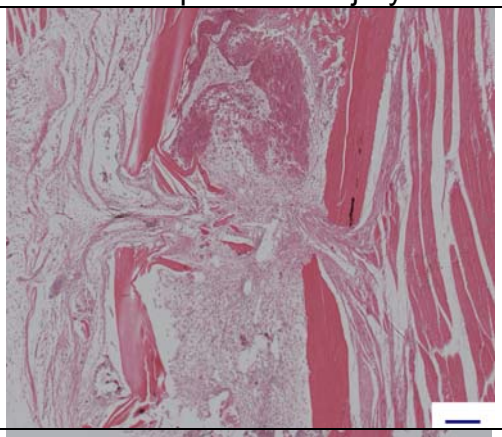
21	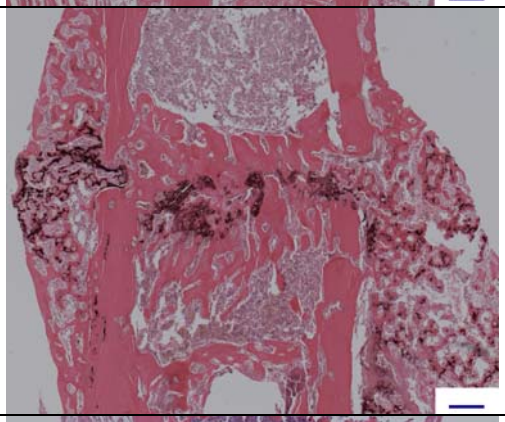	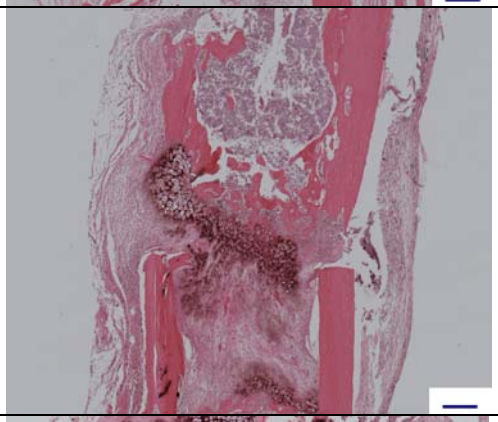
28	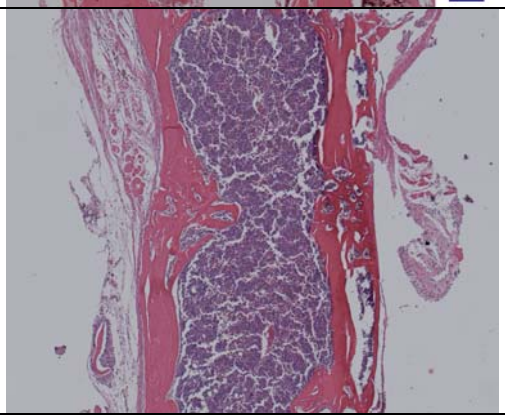	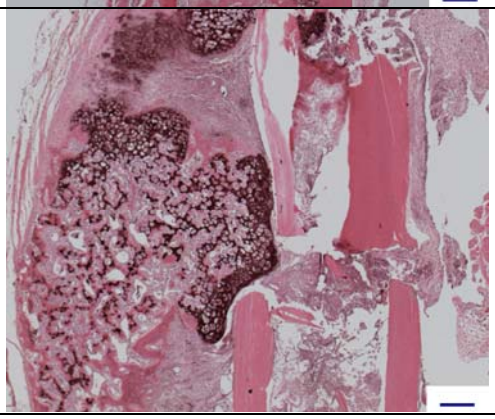

Figure 14: Histology of mid- sagittal section through the osteotomy gap, stained with collagen II + Haematoxylin / Eosin (50x magnification), (blue scale bar: 200 µm).

day	control group	with periosteal injury
14	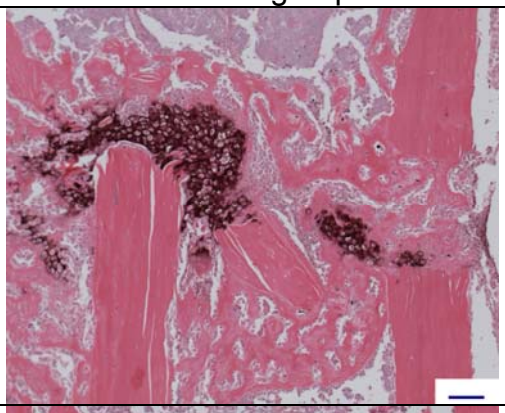	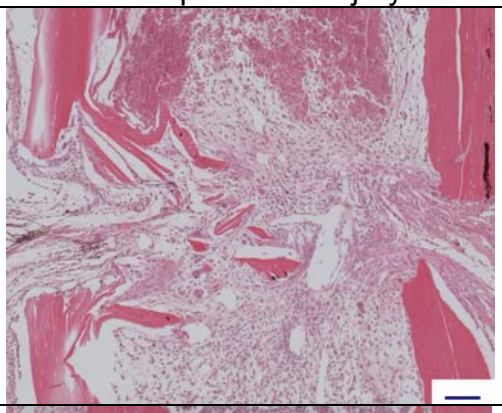
21	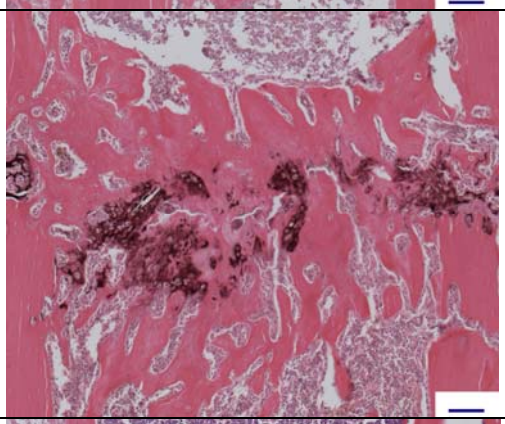	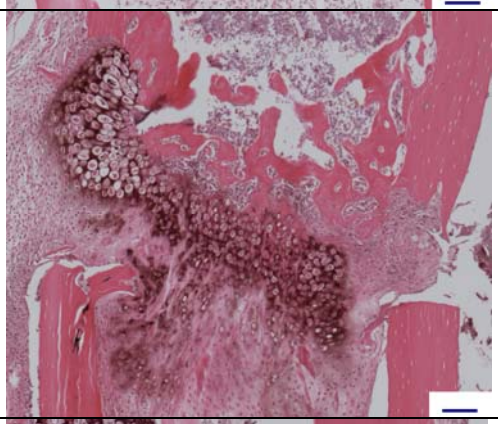
28	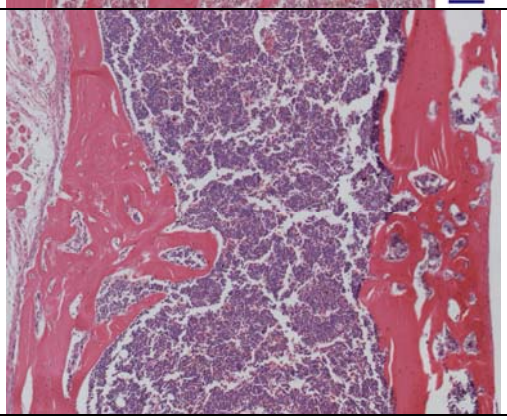	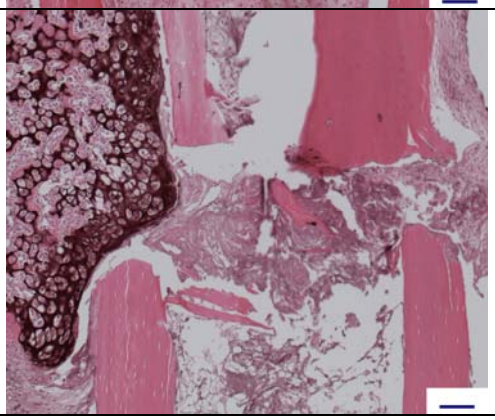

Figure 15: Histology of mid- sagittal section through the osteotomy gap, stained with collagen II + Haematoxylin / Eosin (100x magnification), (blue scale bar: 100 µm).

day	control group	with periosteal injury
14	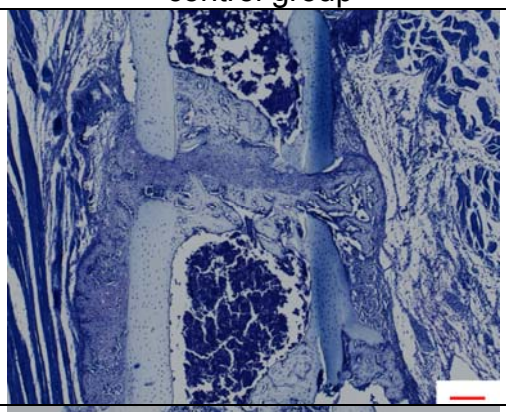	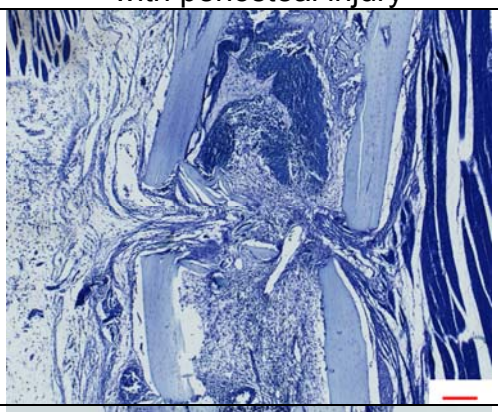
21	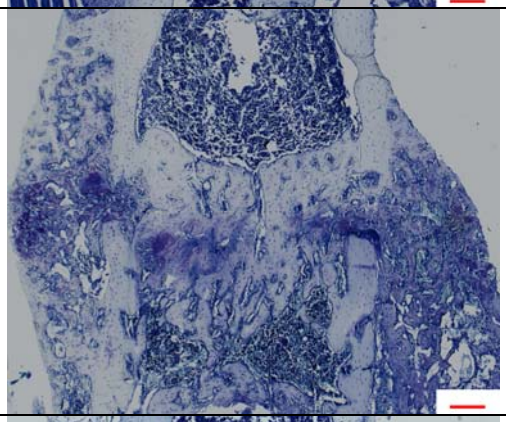	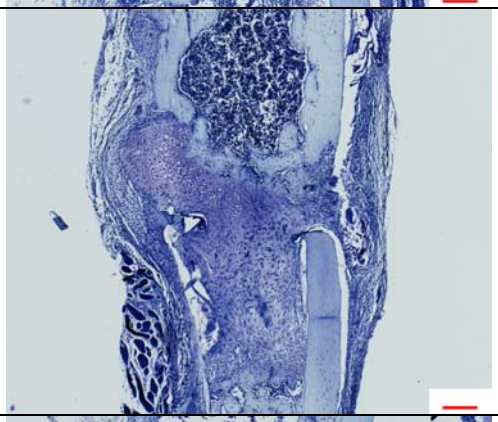
28	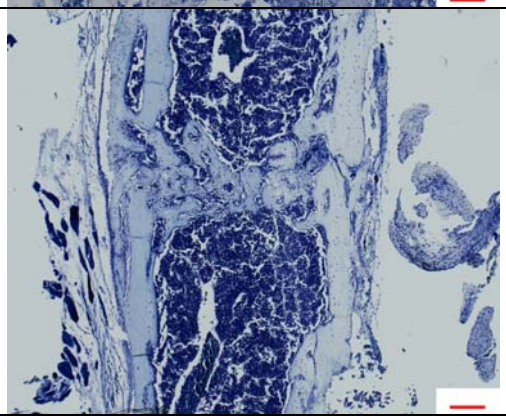	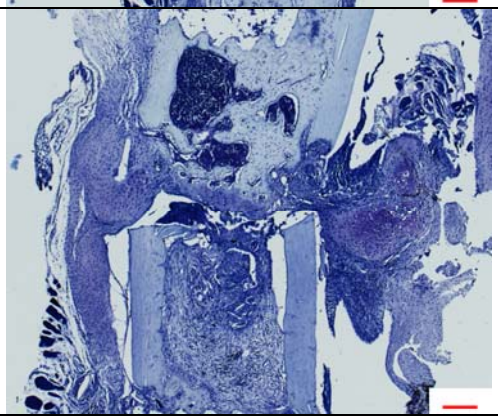

Figure 16: Histology of mid- sagittal section through the osteotomy gap, stained with Toluidine blue (50x magnification), (red scale bar: 200 µm).

day	control group	with periosteal injury
14	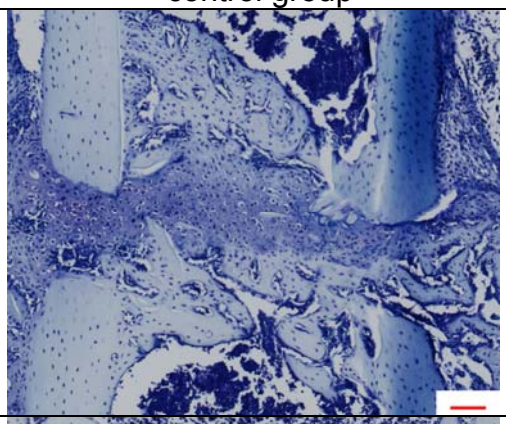	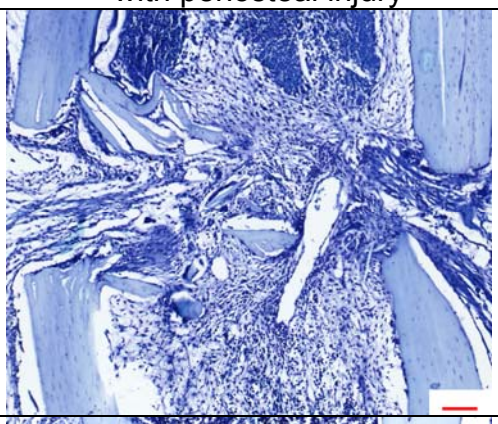
21	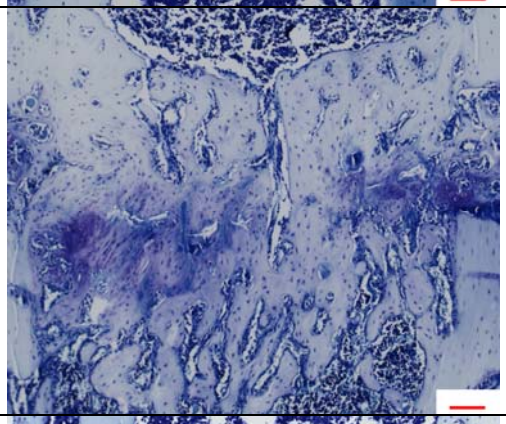	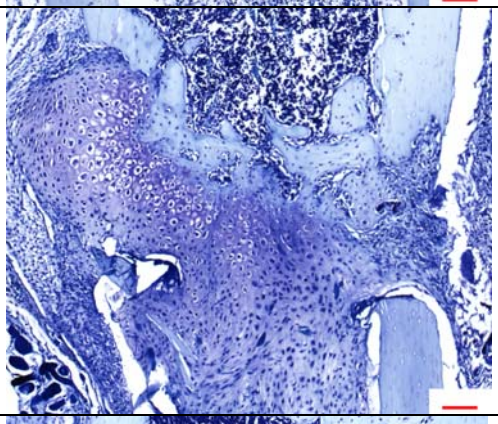
28	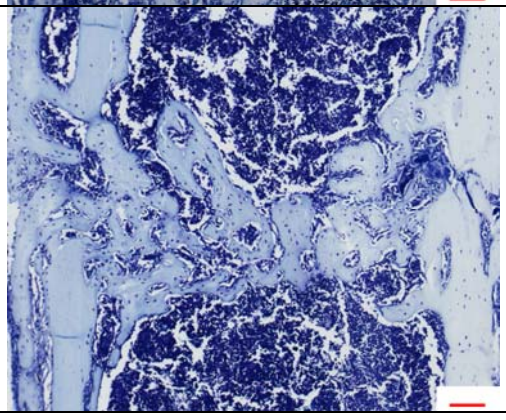	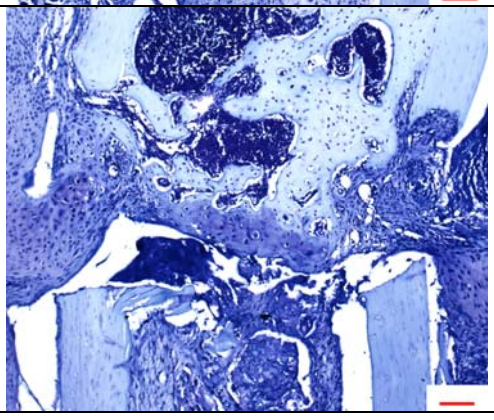

Figure 17: Histology of mid- sagittal section through the osteotomy gap, stained with Toluidine blue (100x magnification), (red scale bar: 100 µm).

DISCUSSION

Interfragmentary instability as well as inadequate blood supply have been claimed as the two major reasons for the development of delayed union [10,13,14,16,17]. The aim of this project was to establish an in vivo murine model for this pathological finding. Our hypothesis was that a fracture gap obtained by osteotomy, reduced with flexible internal fixation in combination with a periosteal injury would lead to a delayed union in mice. The results demonstrated that such experimental approach indeed postponed, i.e. prolonged the healing course for 10 to 15 days. A significant reduction in woven bone formation was attained by cauterization of the periosteum in fracture proximity. While in the control group resorption of the fracture callus via remodeling processes was well advanced showing restoration of the bone diameter, reconstruction of the medullary canal at the end of the experimental period, in the group with periosteal injury only first signs of partial cortical rebridgement were recognizable.

Results from the micro-CT analysis demonstrated that as a consequence of the periosteal injury, the typical healing response to a fracture in the form of a callus was inhibited. The amount of woven bone in and mostly around the gap was significantly reduced, which subsequently seemed to have substantially affected the normal course of healing. The rebridgement of the fragments with more mineralized, lamellar bone was delayed accordingly. The qualitative results from the immuno-histological evaluation also attested to the shift in fracture repair. Monitoring formation, maturation and hypertrophy of chondrocytes using Col II and Col X markers, the delayed progress of endochondral ossification caused by the periosteal injury was assessed. In the control group the physiological sequence of fracture healing took

place consisting of initial stabilization with fibrocartilage callus, subsequent replacement of this structure with woven bone and the gradual resorption and remodeling into lamellar bone. On the contrary, in the group with periosteal damage the normal healing cascade was obviously prolonged due to the fact that at later time-points fibrous connective tissue and cartilage were still present in the gap, chondrocytes had just started to hypertrophy, limited amount of woven bone were present and no complete bridging of the cortices was evident. Consistent outcome was obtained from the mechanical testing: the postponed healing resulted in delayed mechanical functionality. While for both groups bending stiffness increased over time, i.e. a progression was evident for the periosteal injured bones as well, for the control group the advanced stage of healing was noticeable in higher loading capabilities, probably mostly conferred from the larger callus supporting the fracture and from the higher degree in bone mineralization. Finally, the same trend was depicted in the radiographic score, where differences in healing progress were clearly reflected in a delay. Similar scoring for healing was temporarily shifted up to approximately 1-2 weeks in the samples whose periosteum had been cauterized.

Fractures cause the interruption of the medullary as well as the metaphyseal arteries. This leads to reduced blood supply that as a consequence has to be supported by a recruitment of periosteal and extraosseous arteries [10,18,19,20,31]. The periosteum contains osteoblasts and osteoprogenitor cells which equip it with considerable osteogenic potential [32]. The cauterization procedure performed in our study destroyed the periosteum in the gap proximity. This probably led to a reduced release and proliferation of various cell types and to a reduced capacity to form bone and cartilage [17], with consequent failure of appropriate bone healing [19,33]. The critical role of the periosteum explains the fact that in our study in the periosteal

injured group for the first two weeks neither chondrocytes nor osteoblastic-specific cells were migrating to the gap. Thus, only fibrous tissue could develop up to this point. Lack of appropriate fibro-, chondro- and osteoblast progression reduced and retarded the adequate formation of a robust and increasingly mineralized callus. The persistent instability associated with the flexible fixation and insufficient callus formation did not provide the adequate environment for bone forming cell differentiation. The still unstable healing response probably led to the cartilaginous reaction visible after 4 weeks, an attempt to finally support and start normal healing.

Despite that animals and especially small rodents like mice are not an exact model for the human skeleton, several features are similar to the bones of humans, especially the physiological mechanisms of bone modeling and remodeling processes [34]. Moreover, the availability of standardized fixation modules for osteosynthesis (AO Research Implant System, AO Development Institute, Davos, Switzerland) allows better, repeatable and more consistent definition of the loading situation. In our investigation, we did not induce additional pathophysiological problems as for instance in mice models studying the effect of smoke on the healing pattern [23]. Instead, we tried to replicate a situation that could deliver more detailed information on the effect of local blood and cellular supply and at the same time be clinically relevant (e.g. damage of the periosteum in comminuted fractures). The model can be combined with other existing mice models, e.g. studies on osteoporosis based on senescence accelerated mice or any other research effort trying to correlate specific knock-out genes to fracture healing.

In conclusion, a moderate fracture gap performed by osteotomy and fixed by flexible fixation in combination with an additional periosteal injury caused by cauterization could lead to a delayed union in a murine model. The periosteal injury induced a

delay of healing time for up to 1-2 weeks. A similar delay is considered to be clinically relevant since normalized by averaged healing time in mice (4 weeks) [35,36] and humans (16 to 20 weeks) [28], it can be extrapolated that a delay of about 7-10 days in mice would correspond to delayed healing by around 4-6 weeks in humans. In future, this mouse model with periosteal injury can be used to evaluate basic research question regarding delayed unions such as involvement of certain pathways or genes or to develop diagnostic tools and treatment options.

REFERENCES

[1] Urist MR, McLean FC. The local physiology of bone repair with particular reference to the process of new bone formation by induction. Am.J.Surg. 1953;85:444-449.

[2] Gerstenfeld LC et al. Fracture healing as a post-natal developmental process: molecular, spatial, and temporal aspects of its regulation. J.Cell Biochem. 2003;88:873-884.

[3] Dimitriou R, Tsiridis E, Giannoudis PV. Current concepts of molecular aspects of bone healing. Injury 2005;36:1392-1404.

[4] Iwaki A et al. Localization and quantification of proliferating cells during rat fracture repair: detection of proliferating cell nuclear antigen by immunohistochemistry. J.Bone Miner.Res. 1997;12:96-102.

[5] Einhorn TA et al. The expression of cytokine activity by fracture callus. J.Bone Miner.Res. 1995;10:1272-1281.

[6] Colnot C et al. Altered fracture repair in the absence of MMP9. Development 2003;130:4123-4133.

[7] Miclau T et al. Effects of delayed stabilization on fracture healing. J.Orthop.Res. 2007;25:1552-1558.

[8] Praemer A, Furner S, Rice DP. Musculoskeletal conditions in the United States. American Academy of Orthopeadic Surgeons; 1992.

[9] Goldhahn S et al. [Treatment methods and outcomes of tibial shaft fractures in Switzerland. A prospective multicenter study of the Swiss AO]. Swiss.Surg. 2000;6:315-322.

[10] DeAngelis MP. Causes of delayed union and nonunion of fractures. Vet.Clin.North Am. 1975;5:251-258.

[11] McKee MD, Ochsner PE. Aseptic nonunion. In: Rüedi TP, Buckley RE, Moran CG, editors. AO Principles of Fracture Management, Davos: AO Publishing 2007;505-520.

[12] Hayda RA, Brighton CT, Esterhai JL, Jr. Pathophysiology of delayed healing. Clin.Orthop.Relat Res. 1998;S31-S40.

[13] Sarmiento A et al. Fracture healing in rat femora as affected by functional weight-bearing. J.Bone Joint Surg.Am. 1977;59:369-375.

[14] Glowacki J. Angiogenesis in fracture repair. Clin.Orthop.Relat Res. 1998;S82-S89.

[15] Carter DR, Blenman PR, Beaupre GS. Correlations between mechanical stress history and tissue differentiation in initial fracture healing. J.Orthop.Res. 1988;6:736-748.

[16] Brinker MR, Bailey DE, Jr. Fracture healing in tibia fractures with an associated vascular injury. J.Trauma 1997;42:11-19.

[17] Lu C et al. Ischemia leads to delayed union during fracture healing: a mouse model. J.Orthop.Res. 2007;25:51-61.

[18] Dickson KF, Katzman S, Paiement G. The importance of the blood supply in the healing of tibial fractures. Contemp.Orthop. 1995;30:489-493.

[19] Cornell CN, Lane JM. Newest factors in fracture healing. Clin.Orthop.Relat Res. 1992;297-311.

[20] Trueta J. Blood supply and the rate of healing of tibial fractures. Clin.Orthop.Relat Res. 1974;11-26.

[21] Einhorn TA. The cell and molecular biology of fracture healing. Clin.Orthop.Relat Res. 1998;S7-21.

[22] Garcia P et al. A new technique for internal fixation of femoral fractures in mice: impact of stability on fracture healing. J.Biomech. 2008;41:1689-1696.

[23] El Zawawy HB et al. Smoking delays chondrogenesis in a mouse model of closed tibial fracture healing. J.Orthop.Res. 2006;24:2150-2158.

[24] Duvall CL et al. Impaired angiogenesis, early callus formation, and late stage remodeling in fracture healing of osteopontin-deficient mice. J.Bone Miner.Res. 2007;22:286-297.

[25] Yang X et al. Callus mineralization and maturation are delayed during fracture healing in interleukin-6 knockout mice. Bone 2007;41:928-936.

[26] Groengroeft ID et al. Fixation compliance in a murine fracture model induces two different processes of frature healing but does not lead to delayed union. 6th Combined Meeting of the Orthopaedic Research Societies, Honolulu (Hawai, USA) 2007; paper 138.

[27] Matthys-Mark R, Perren SM. Technical note: The MouseFix-system. Unpublished data 2007.

[28] Ito K, Perren SM. Biology and biomechanics in bone healing. In: Rüedi TP, Buckley RE, Moran CG, editors. AO Principles of Fracture Management, Davos: AO Publishing 2007;9-33.

[29] Gabet Y et al. Osteogenic growth peptide modulates fracture callus structural and mechanical properties. Bone 2004;35:65-73.

[30] Garrett IR et al. Locally delivered lovastatin nanoparticles enhance fracture healing in rats. J.Orthop.Res. 2007;25:1351-1357.

[31] Macnab I, De Haas WG. The role of periosteal blood supply in the healing of fractures of the tibia. Clin.Orthop.Relat Res. 1974;27-33.

[32] Mc Lean FC, Urist MR. Bone. The University of Chicago Press, Chicago (Illinois, USA) 1955;Third Edition (1968).

[33] Claes L, Eckert-Hubner K, Augat P. The effect of mechanical stability on local vascularization and tissue differentiation in callus healing. J.Orthop.Res. 2002;20:1099-1105.

[34] Utvag SE, Grundnes O, Reikeraos O. Effects of periosteal stripping on healing of segmental fractures in rats. J.Orthop.Trauma 1996;10:279-284.

[35] Bourque WT, Gross M, Hall BK. A reproducible method for producing and quantifying the stages of fracture repair. Lab Anim Sci. 1992;42:369-374.

[36] Hiltunen A, Vuorio E, Aro HT. A standardized experimental fracture in the mouse tibia. J.Orthop.Res. 1993;11:305-312.

ACKNOWLEDGEMENTS

I am very thankful that the AO Research Institute gave me the possibility to conduct my doctoral thesis at their institution. I would like to thank my academic supervisor Prof. Pierre Montavon, as well as Prof. Keita Ito and Dr. Andrea Tami for their direct supervision during the study. As far as the histological work is concerned, I would like to thank Dr. Stefan Milz and his team for supporting me, Christoph Sprecher for the technical aid with image analysis and Dr. Ina Groengroeft for preparing this project and carrying out the surgeries. Last but not least I would like to thank my family and friends for giving me their support.

Lebenslauf

Name	Sandra Wissing
Geburtsdatum	30.03.1979
Geburtsort	Hagen (Deutschland)
Nationalität	Deutsch

1985 – 1989	Grundschule Haste, Osnabrück (Deutschland)
1989 – 1991	Thomas-Morus-Schule (Orientierungsstufe), Osnabrück (Deutschland)
1991 – 1998	Angelaschule Osnabrück (Staatlich anerkanntes Gymnasium der Schulstiftung im Bistum Osnabrück), Osnabrück (Deutschland)
1998	Abitur
1998 – 1999	Lehrgang „Grundzüge der Naturheilkunde“, Münster (Deutschland)
1999 – 2001	Ausbildung zur Biologisch-Technischen-Assistentin, Osnabrück (Deutschland)
2001	Staatlich anerkannte Biologisch-Technische-Assistentin
2001 – 2002	Studium der Veterinärmedizin an der Szent Istvan Fakultät der Universität Budapest, Budapest (Ungarn)
2002 – 2007	Studium der Veterinärmedizin an der Veterinärmedizinischen Fakultät der Universität Leipzig, Leipzig (Deutschland)
2007	Approbation an der Veterinärmedizinischen Fakultät der Universität Leipzig, Leipzig (Deutschland)
2007 – 2008	Wissenschaftliche Mitarbeiterin und Doktorandin am AO Forschungsinstitut, Davos (Schweiz) und an der Vetsuisse-Fakultät der Universität Zürich, Zürich (Schweiz)

16.10.2008